

# Prospects of shale gas exploitation in Lower Gondwana of Raniganj Coalfield (West Bengal), India

SUBHASHREE MISHRA<sup>1</sup>, VINOD A. MENDHE<sup>1\*</sup>, ALKA D. KAMBLE<sup>1</sup>,  
MOLLIKA BANNERJEE<sup>1</sup>, ATUL K. VARMA<sup>2</sup>, BHAGWAN D. SINGH<sup>3</sup>  
AND JAI K. PANDEY<sup>1</sup>

<sup>1</sup>CSIR–Central Institute of Mining and Fuel Research, Dhanbad 826 015, Jharkhand, India.

<sup>2</sup>Department of Applied Geology, Indian School of Mines, Dhanbad 826 004, Jharkhand, India.

<sup>3</sup>Birbal Sahni Institute of Palaeobotany, 53 University Road, Lucknow 226 007, India.

\*Corresponding author: vamendhe@gmail.com

(Received 20 July, 2015; revised version accepted 08 February, 2016)

## ABSTRACT

Mishra S, Mendhe VA, Kamble AD, Bannerjee M, Varma AK, Singh BD & Pandey JK 2016. Prospects of shale gas exploitation in Lower Gondwana of Raniganj Coalfield (West Bengal), India. The Palaeobotanist 65(1): 31–46.

Geochemical analyses such as proximate, pyrolysis, TOC and FTIR, and other analyses like surface area, pore size, pore volume (using low–pressure N<sub>2</sub> physisorption measurements) and SEM were performed on the shale samples derived from Early Permian Barakar and Late Permian Barren Measures formations of the Raniganj Coalfield, West Bengal. Rock–Eval pyrolysis and TOC data indicated that the heterogeneity of Barren Measures and Barakar shales is laterally varying, but in general, factors which support the occurrence of shale gas accumulations include a moderate to high TOC content (3.38–7.87 wt.%) with sufficient thermal maturity and type III–IV organic matters (kerogens). FTIR spectra indicate the presence of quartz and kaolinite with absorbance bandwidth between 1200–800 cm<sup>-1</sup> and 3750–3400 cm<sup>-1</sup>, respectively. Abundance of quartz, as compared to clay, points towards the brittle characteristics of shales favourable for good fracability. Besides, mesopores and macropores are well–developed and the capacity of gas generation and adsorption are significant.

On the basis of SEM, the pores are classified into four types– (i) inter–granular pores, (ii) dissolve pores, (iii) composite inter–granular pores, and (iv) hair line micro–fractures. The BET multipoint surface area varies from 8.104 to 16.937 m<sup>2</sup>/g and 17.376 to 29.675 m<sup>2</sup>/g for Barakar and Barren Measures shales, respectively. Size of the pores varies from 3.072 to 3.728 nm for the Barakar shales and 2.984 to 3.521 nm for the Barren Measures shales, as measured by BJH method. Overall, it is observed that mesopores, macropores, micro–fractures and micropores are adequate in the samples and the studied shales are having interconnected networks of natural cracks and pores system, which may control the storage and migration of shale gas in the reservoir.

**Key–words**—Permian shales, Rock–Eval pyrolysis, Thermal maturity, Pore structures, Adsorption–desorption isotherm, Hydrocarbon potential.

रानीगंज कोयलाक्षेत्र (पश्चिम बंगाल), भारत के अधो गोंडवाना में शेल गैस स्वार्थसाधन की संभावनाएं  
सुभाश्री मिश्र, विनोद ए. मेंडे, अलका डी. कांबले, मॉल्लिका बैनर्जी, अतुल के. वर्मा, भगवान डी. सिंह एवं जय के. पांडे

## सारांश

रानीगंज कोयलाक्षेत्र, पश्चिम बंगाल के प्रारंभिक पर्मियन बराकार एवं विलंबित पर्मियन अनुत्पादक शैल–संस्तर शैलसमूहों से व्युत्पन्न शेल नमूनों पर भू–रासायनिक विश्लेषण जैसे घटक–वर्ग, तापांशन, टी ओ सी एवं एफ टी आई आर तथा पृष्ठीय क्षेत्र, छिद्रिल आकार, छिद्रिल आयतन (अल्प दबाव N<sub>2</sub> भौतिक शोषण मापन प्रयुक्त करते हुए) और क्रमवीक्षण इलेक्ट्रॉन सूक्ष्मदर्शी जैसे अन्य विश्लेषण किए गए। शैल–मूल्यांकन तापांशन एवं टी ओ सी आंकड़े ने संकेत दिया कि अनुत्पादक शैल–संस्तरों एवं बराकार शैलों की विजातीयता पार्श्व रूप से परिवर्तित है किंतु व्यापक रूप से, पर्याप्त तापीय परिपक्वता एवं III–IV प्रकार कार्बनिक पदार्थों (कैरोजन) सहित मध्यम से उच्च टी ओ सी अंतर्वस्तु (3.38–7.87 भार %) समाविष्ट शेल गैस संचयन समर्थन प्रदान करते हैं। एफ टी आई आर स्पेक्ट्रा क्रमशः 1200–800 सेमी<sup>-1</sup> एवं 3750–3400 सेमी

<sup>1</sup> के मध्य अवशोषणांक बैंड की चौड़ाई सहित क्वार्टज़ व कैवलीनाइट की विद्यमानता इंगित करते हैं। मृदा की तुलना में क्वार्टज़ की बहुलता अच्छे परासूक्ष्मदरार हेतु अनुकूल शैलों के भंगुर अभिलक्षणों की ओर इंगित करती है। इसके अलावा, मध्य रंध्र व स्थूल रंध्र सुविकसित हैं तथा गैस उत्पादन एवं अवशोषण की क्षमता महत्वपूर्ण हैं।

क्रमवीक्षण इलेक्ट्रान सूक्ष्मदर्शी के आधार पर रंध्र चार प्रकारों में वर्गीकृत हैं— 1) अंतः-कणिकामय रंध्र, 2) विलीन रंध्र, 3) संयुक्त अंतःकणिकामय रंध्र, एवं 4) केशिका सूक्ष्म-भंजन। बी ई टी बहुबिंदु पृष्ठीय क्षेत्र क्रमशः बराकार और अनुत्पादक शैल-संस्तर शैलों हेतु 8.104 से 16.937 m<sup>2</sup>/g और 17.376 से 29.675 m<sup>2</sup>/g तक भिन्न-भिन्न हैं। बी जे एच विधि से यथा मापित बराकार शैलों हेतु 3.072 से 3.728 nm तक और अनुत्पादक शैल-संस्तर शैलों हेतु 2.984 से 3.521 nm तक छिद्रिलों का आकार बदलता है। कुल मिलाकर देखा गया है कि नमूनों में मध्य रंध्र, स्थूल रंध्र, सूक्ष्म दरार एवं सूक्ष्म रंध्र पर्याप्त हैं तथा अध्ययन किए शैल प्राकृतिक दरारों एवं छिद्र समूह के अंतर्संबद्ध जालक्रमों से युक्त हैं, जो भण्डार में शैल गैस के संचयन एवं विस्थापन को नियंत्रित कर सकते हैं।

**सूचक शब्द**— पर्मियन शेल्स, शैल मूल्यांकन तापांशन, तापीय परिपक्वता, छिद्र संरचनाएं, अवशोषण-विशोषण समताप रेखा, हाइड्रोकार्बन संभावना।

## INTRODUCTION

SHALE is most common sedimentary rock composed of fine-grained detrital material such as sand and silt sized particles of quartz and flakes of clay, and 5 to 20% of organic matter (Guarnone *et al.*, 2012; Kuila & Prasad, 2013). Examination of shale attributes has increased dramatically since shale gas systems have become commercially hydrocarbon production targets (Jarvie *et al.*, 2001, 2007; Rowe *et al.*, 2008; Loucks *et al.*, 2009). Shale gases are unconventional gas systems in which the shale is both the source and the reservoir rocks for methane (CH<sub>4</sub>), which is derived from the organic matters within the shale through biogenic and/or thermogenic processes (Hill *et al.*, 2007; Strapoc *et al.*, 2010). In terms of chemical composition, shale gases are typically a dry gas, composed primarily of methane (by volume 65–95%), but some sequences do produce wet gas that depends on maturity of shale deposits (Mendhe *et al.*, 2015a). The combination of horizontal drilling and hydraulic fracturing has allowed access to large volumes of shale gases that were previously uneconomical to produce.

Natural gas stored in the shale reservoirs is held in one of three forms—(i) free gas in pores and natural fractures, (ii) sorbed gas in organic matter and on inorganic clay minerals, and (iii) dissolved gas in oil and water (Zhang *et al.*, 2012; Yang *et al.*, 2014; Yuguang *et al.*, 2014; Varma *et al.*, 2015a). The shale has low porosity and intrinsically low permeability (< 0.1 nD) as compared to most of the conventional reservoirs like sandstone, limestone or dolomite (Schlömer & Krooss, 1997; Li *et al.*, 2005; Mendhe *et al.*, 2015a). As per the International Union of Pure and Applied Chemistry (IUPAC) classification, pores are generally ranging from micropores (pore diameter < 2 nm), mesopores (2–50 nm), and macropores (pore diameter > 50 nm). The hydrocarbon generation potential of shale horizons depends on the amount, type and maturity of organic matter (kerogen) present in it (Tissot & Welte, 1984; Sykes & Snowdon, 2002). Rock-Eval pyrolysis and total organic carbon (TOC) are the most widely

used parameters for the characterization of hydrocarbons (oil/gas) generation potentiality of the shale beds (Espitalié *et al.*, 1977; Peters, 1986; Varma *et al.*, 2011, 2015a, b).

India has laid out an ambitious strategy for developing its vast shale gas resources. At the foremost, Lower Gondwana (Permian) shale deposits in the Raniganj Coalfield show good exploration prospects (Mendhe *et al.*, 2015a). Varma *et al.* (2011) evaluated the shales through TOC-pyrolysis, ultimate (CHNSO) and petrographic analyses for their hydrocarbon generation potential from the eastern part of coalfield. Varma *et al.* (2014, 2015b) further accessed the organic richness and sorption dynamics in relation to hydrocarbons prospect, and concluded that the shales are of good to excellent TOC contents with chiefly type III organic matter. They placed the shales within the estimated vitrinite reflectance 'oil window', capable of generating oil and thermogenic gas (CH<sub>4</sub>) upon thermal cracking. The Langmuir volume points towards positive role of organic matter and clay association in shale gas adsorption (Hazra *et al.*, 2015; Varma *et al.*, 2015c). The kerogen (organic matter) abundance is found to be a significant factor, as indicated by good correlations between TOC content and sorption amount, in controlling methane (gas) sorption for the shales of Raniganj Coalfield.

In view, limited researches and pilot scale exploration work for shale gas resources have been undertaken in the promising Raniganj Coalfield. The aim of present study is to characterize the subsurface Early and Late Permian shales belonging to Barakar and Barren Measures formations, respectively from the north-western part of the coalfield on the basis of TOC contents, kerogen/organic matter types, thermal maturity, surface area, pore size, pore volume, categorization of pores (under SEM), and Fourier Transform Infrared (FTIR) spectroscopy and proximate analyses (for geochemical parameters). The results of experimental findings have important implications for shale gas explorations, resource assessments and recovery technologies in the Raniganj Coalfield.

**RANIGANJ COALFIELD**

The Raniganj Coalfield has abundant hydrocarbons potentiality and currently most active coal bed methane (CBM) producing region in India. It is a sole repository of different types of superior quality, high-volatile and non-coking coals. The coalfield is the easternmost depository within the Damodar Valley of Gondwana basins (Ghosh, 2002). The Raniganj Coalfield has a semi-elliptical, elongated shape and covers an area of about 1,600 km<sup>2</sup> spreading over Burdwan, Birbhum, Bankura and Purulia districts in West Bengal, and Dhanbad District in Jharkhand states. The most prospective part of the coalfield, however, falls in Burdwan District. The coalfield is bounded by the Ajay River in north and by the Damodar River in south and lies within the latitudes 23°22' & 23°52' N and longitudes 86°36' & 87°30' E (Gee, 1932). Two major faults traverse the area, one orienting NNE–SSW in the western part, and the other in NNW–SSE direction in the eastern part (Dutt, 2003). The Raniganj Coalfield is intersected by numerous igneous intrusions of dolerites/basalts and lamprophyres.

The coalfield contains Gondwana sediments right from Talchir (Early Permian) to Panchet (Triassic) formations (Fig. 1). The greater part of the Raniganj Coalfield is covered by Lower Gondwana sediments of Permian age. These sediments unconformably overlie the basement Precambrian rocks and have many economic coal seams and huge shale deposits. The basal part of the Lower Gondwana sediments is represented by Talchir Formation and is succeeded gradationally by Barakar (Early Permian), Barren Measures (early Late Permian) and Raniganj (Late Permian) formations. The Permian sediments are overlain by the Panchet Formation (Triassic) in the area. The coal-bearing Raniganj Formation exhibits its maximum development in this coalfield and attains a maximum thickness of about 1,150 m. The formation houses more than two-thirds of the coal reserves. In addition, the Barakar Formation is also an important coal contributor in the Raniganj Coalfield. In general, lithology of coal-bearing sequences in the coalfield is represented by course- to medium-grained sandstones with siltstones, carbonaceous and grey shales and coal seams (Gupta *et al.*, 2012). The general lithostratigraphic succession of the Raniganj Coalfield compiled from Ghosh (2002), Dutt (2003) and Mukhopadhyay *et al.* (2010) is given in Table 1.

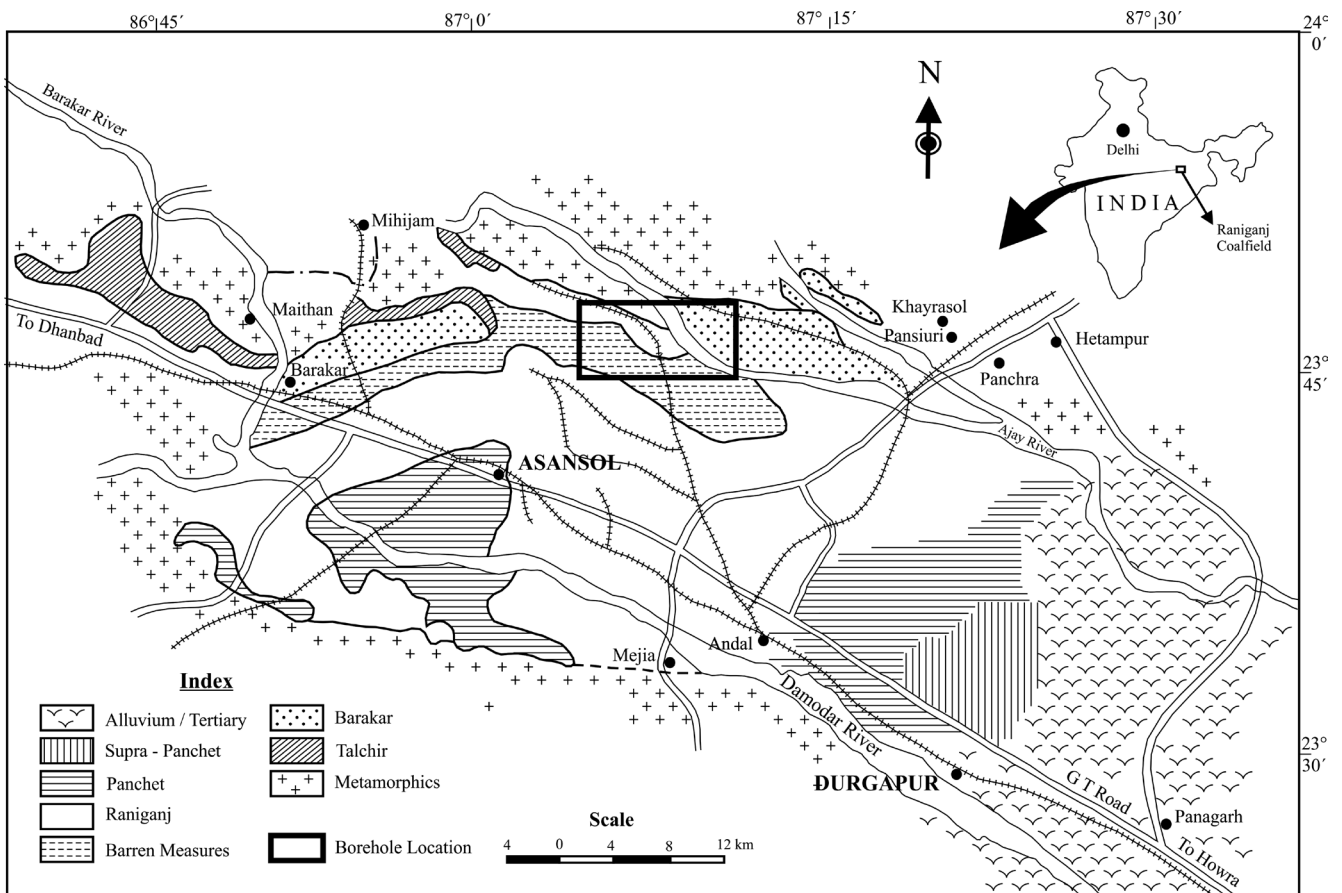


Fig. 1—Geological map of the Raniganj Coalfield, India (source: Dutt, 2003), marked with sampling borehole sites.

Table 1—Generalized stratigraphic succession of the Raniganj Coalfield.

Age	Formation	Lithology	Thickness
Recent & Quaternary	Surficial deposits	Top soil—alluvium & sandy soil	20 m
		—————Unconformity—————	
Tertiary	—	Loose sand, lateritic gravel, clayey sandstone, mudstone, siltstone with bands of marlstone and mottled clay	300 m
		—————Unconformity—————	
Cretaceous	Igneous intrusive	Basic (dolerite) dykes, ultrabasic (mica-peridotite, mica-lamprophyre, lamprophyre) sills and dykes	—
Cretaceous	Rajmahal	Greenish grey to black, fine- to medium-grained vesicular porphyritic basalt and volcanic breccia, fine-grained sandstone, carbonaceous and grey shales	120 m
		—————Unconformity—————	
Late Triassic	Supra Panchet/ Durgapur beds	Massive, coarse-grained red and grey quartzose sandstones, conglomerate with dark grey silty shale bands	300 m
		—————?Unconformity—————	
Early Triassic	Panchet	Coarse-grained greenish yellow and greenish grey soft, micaceous, cross bedded sandstone with slump structure, khaki green fissile silty shale, conglomerates at the base	600 m
		—————Unconformity—————	
Late Permian	Raniganj	Fine- to medium-grained micaceous feldspathic grey and greenish sandstones with shales and coal seams	520–1150 m
Late Permian	Barren Measures	Carbonaceous fissile shales with bands of sandy micaceous shales and clay iron stone	400–600 m
Early Permian	Barakar	Coarse- to medium-grained, arkosic, white and grey sandstones, grey and carbonaceous shales, coal seams and fireclay lenses	600–750 m
Early Permian	Talchir	Coarse-grained sandstone, white/ slight variegated green shales and fine-grained sandstone with un-decomposed feldspar & boulder beds at the base	200–500 m
		—————Unconformity—————	
Precambrian	Chotanagpur Complex	Granite gneiss with magmatite gneiss, hornblende schist/gneiss, meta-basic rocks, pegmatite and quartz veins	—

### SHALE OCCURRENCES

In Permian Lower Gondwana sequence of the Raniganj Coalfield, the major shale-bearing formation is Barren Measures, which has laterally varying thickness of about 400 to 600 m. The coal-bearing Barakar and Raniganj formations also contain thick shale beds. The Barakar Formation upwards, into a sequence of monotonous dark grey and black shales with bands and lenses of hard, fine-grained, cryptocrystalline clay ironstone, was originally termed 'Ironstone shale' or Barren Measures (Blanford, 1861; Fox, 1928). However, the Barren Measures includes a thick black and carbonaceous shale sequence in the middle with sandstone and shale sequence

below and a sandstone horizon above. The Barren Measures shale is best developed in the western part of coalfield, where a cumulative thickness of the formation is around 600 m as estimated from boreholes data. In boreholes drilled through the Raniganj Formation to the south of Damodar River, the thickness of Barren Measures has been recorded to be over 700 m (Majumdar *et al.*, 1977). The attenuation of the thickness of the formation to the east has not been marked. In the eastern part, about 475 m of Barren Measures Formation has been recorded in subsurface. The formation is developed in an east-west elongated stretch, more or less parallel to the Barakar Formation.

The Barakar Formation shows its zenith of development in the western and northern parts of the Raniganj Coalfield, and gradually thins down towards east and south (Dutt, 2003). The estimated maximum thickness of Barakar strata is of the order of 750 m. The arenaceous sediments of the Barakar Formation on the whole, are coarser than those of the other formations of Lower Gondwana sequence. The dominant sediments of the Barakar Formation are sandstone, carbonaceous shale and coal. The bulk of the sandstone is highly feldspathic, and the matrix is generally clayey, probably derived from kaolinite feldspar. The sandstone and shale, usually deposited as lensoid bodies, are highly cross-bedded, slumped, convoluted and deformed. They are inter-layered with micaceous shaly sandstones, sandy shales, grey shales, carbonaceous shales, fireclay and coal seams of variable thickness. The presence of thick and widespread shales in both the Barakar and Barren Measures formations and high rock fragility indicates a stable and deep-water environmental condition during the shale deposition in Raniganj Coalfield (Dutt, 2003).

### SAMPLING AND ANALYTICAL TECHNIQUES

**Collection of samples**—Total eight shale core samples were collected (4 each) from the Barakar and Barren Measures formations during the exploratory drilling in Dharma area of the Raniganj Coalfield. The sampling site is marked and shown in Fig. 1. The megascopic properties of samples were examined and photographed at the drilling site. Some of the shale core samples are illustrated in Fig. 2, showing physical variations in their banding. The fractured surfaces of samples are uneven to sub-conchoidal.

**Proximate analysis**—Shale samples were analyzed for proximate constituents, such as in-situ moisture content, inorganic ash yield, volatile matter yield and fixed carbon

content, following the standard laboratory procedure as set down by Bureau of Indian Standard (BIS, 1995) to correlate the samples on received and dry ash-free basis. The analyses were performed by taking 70 mesh size powders of representative samples, and using micro-balance, oven (for moisture content) and muffle furnace (for ash and volatile matter yields). Fixed carbon contents in the studied samples are calculated by subtracting the sum of ash yield, volatile matter yield and moisture content from 100.

**Rock-Eval pyrolysis and TOC analysis**—The Rock-Eval pyrolysis experiment and total organic carbon (TOC) content determination were performed using Vinci Technologies®-Rock-Eval 6 Plus TOC Module system, and as per the procedure described by Lafargue *et al.* (1998). The pyrolysis technique consists of a programmed temperature heating (in a pyrolysis oven) of a small amount of rock in an inert atmosphere (helium or nitrogen), and the residual carbon was subsequently burnt in an oxidation oven. The technique helps to determine the amount of hydrocarbons released during pyrolysis, which was detected with a flame ionization detector, while online infrared detectors measure continuously the released carbon mono- and dioxide.

About 1 to 2 gm of shale samples (crushed in < 150 mesh size) were first pyrolysed from 100 °C to 550 °C at a rate of 25 °C/min. The oxidation phase starts with an isothermal stage at 400 °C, followed by an increase to 850 °C at a rate of 25 °C/min to burn out all the residual carbon. The results obtained include the quantity of free hydrocarbons present in the sample (S1 peak), the amount of remaining hydrocarbon compounds (S2 peak), the CO<sub>2</sub> as oxygen containing compounds (S3 peak), the TOC content, and the T<sub>max</sub> (temperature at which the maximum amounts of hydrocarbons are generated). The other parameters calculated from the pyrolysis data are—hydrogen index, oxygen index, production index, hydrogen type index, potential yield, vitrinite reflectance, etc. (Ekweozor & Gormly, 1983; Jarvie *et al.*, 2001, 2005; Ogala, 2011).

**FTIR Spectrometry analysis**—Fourier Transform Infrared (FTIR) spectroscopy of shale samples were carried out using Vertex 80 FTIR system. Samples were crushed in sieve size of 212 µm, and about 1 mg of representative samples was used for the preparation of pellets. The pellet was grounded with 100 mg potassium bromide (KBr), and then pressed the pellet in an evacuated die, following the standard procedures outlined by Painter *et al.* (1981). Prior to analysis, the pellets were kept for dry in a vacuum oven for 48 hours to minimize the contribution of water to the spectrum. The recorded peak assignments are based on the work of Painter *et al.* (1981, 1985), Guo & Bustin (1998), Chen *et al.* (2014), etc.

**SEM analysis**—The Scanning Electron Microscope of Carl Zeiss make was used for the examination and analysis of the micro-structural characteristics and clay minerals present in the studied shale samples. Different pore geometries and components have been identified under the SEM and by the

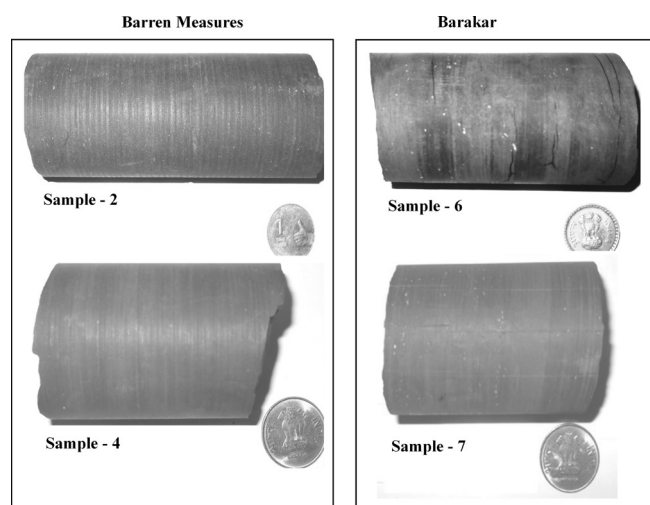


Fig. 2—Core samples of some investigated shales from the Raniganj Coalfield.

energy dispersive X-ray (EDX) analysis of cross sectioned surfaces of the shales.

**Pore structure analysis**—Low-pressure nitrogen ( $N_2$ ) adsorption experiments were conducted using Quantachrome AutosorbIQ™ 2MP–XR system to determine the surface area, pore size and pore volume. Through the application of sub-critical  $N_2$  gas adsorption, the acquired analytical data has indicated capacity as well as revealed information about surface area and pore volume and distribution. About 30 to 40 mg of prepared shale samples (crushed in size of 0.8–1 mm) were taken using high precision balance, and samples were allowed to outgas at 300 °C for 3–4 hours ensuring the removal of bound water adsorbed in the samples. Reagent grade (99.995)  $N_2$  gas was used as adsorbent at liquid nitrogen temperature (-195.79 °C or 77.35 K), and adsorption–desorption isotherms were obtained under relative pressures (P/Po) ranging from 0.05 to 0.1. The Brunauer Emmet Teller (BET) and Barrett–Joyner–Halenda (BJH) Theory, and Density Functional Theory (DFT) are adopted for interpretation of  $N_2$  adsorption–desorption data (Kuila *et al.*, 2012; Quantachrome, 2014; Mendhe *et al.*, 2015a).

## RESULTS AND DISCUSSION

The investigated shale core samples are light to dark grey in colour having alternate bands of grey and carbonaceous-rich material (Fig. 2). The specific gravity of the samples is  $> 2.5$ , dominantly containing clay minerals and visible grains of quartz and mica flakes. The shales of the Early Permian Barakar Formation are mostly medium-grained with flakes of mica. However, the Barren Measures (Late Permian) shales are fine- to medium-grained mostly composed of clay (mud) and quartz/mica flakes; indicating fissile structures.

Proximate analysis is the conventional geochemical analysis carried out to determine the physico-chemical constituents of an organic-rich deposit. The data derived not only determines the suitability of deposits for various industrial uses, but also provides information on the geological history of the sequences and individual horizons (Ward, 2002). Table 2 summarizes the data obtained from proximate analysis

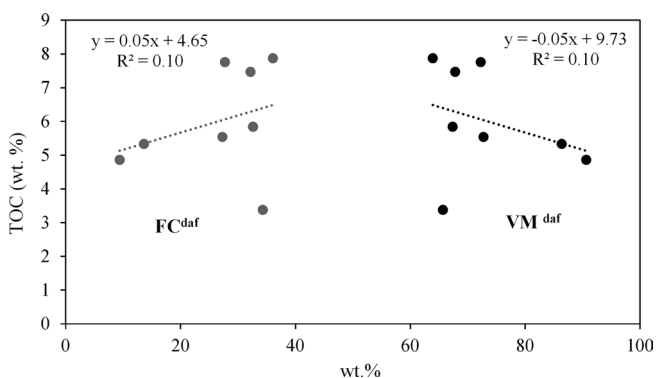


Fig. 3—Relationships between  $VM^{daf}$  and  $FC^{daf}$  vs. TOC of the shale samples.

of air-dried shale samples along with calculated values of volatile matter (VM) and fixed carbon (FC) contents on dry ash-free (daf) basis. The samples contain low total moisture contents (1.19–2.60 wt.%) and high ash yields (82.28–86.33 wt.%). The high ash content is confirming the dominance of minerals in the studied samples. The VM yields and FC contents vary from 8.62 to 11.55 wt.% (daf: 63.92–86.39 wt.%) and 1.17 to 5.64 wt.% (daf: 9.38–36.08 wt.%), respectively in the samples.

The relationships between  $VM^{daf}$  and  $FC^{daf}$  and total organic carbon (TOC; determined via the Rock–Eval pyrolyser, discussed later) extends through the entire samples is shown in Fig. 3. It may be observed that TOC content is gradually increasing with decrease in volatile matter yields (negative trend), while fixed carbon values are in accordance with TOC values. The TOC contents in the samples also increase with increasing fixed carbon contents; establishing a general positive trend with weak linear relationship (Mendhe *et al.*, 2015b). Figure 4 (ash content vs. VM & TOC) illustrates the negative correlation between volatile matter yield and TOC content with respect to ash content of the shales.

The characterization of organic matters from the sedimentary rocks is one of the main objectives of the organic geochemistry, and is now widely recognized as a critical step in the evaluation of hydrocarbon potentials of the sequences. During the last four decades various researchers have used pyrolysis methods to provide data on the potential, maturity and type of the source rocks in different sedimentary basins of the world (Barker, 1974; Claypool & Reed, 1976; Clementz *et al.*, 1979; Espitaliè *et al.*, 1977, 1984; Larter & Douglas, 1982; Horsfield, 1985; Peters, 1986; Peters & Cassa, 1994; Nicholas *et al.*, 2004; Hakimi *et al.*, 2013; Mendhe *et al.*, 2015b; many more). The Rock–Eval and TOC analytical results of organic-rich deposits are used to evaluate the hydrocarbon source rocks and oil and/or gas generation potentials with excellent degree of accuracy (Peters, 1986; Peters & Cassa, 1994; Lafargue *et al.*, 1998; Varma *et al.*, 2011, 2015a, b; Hazra *et*

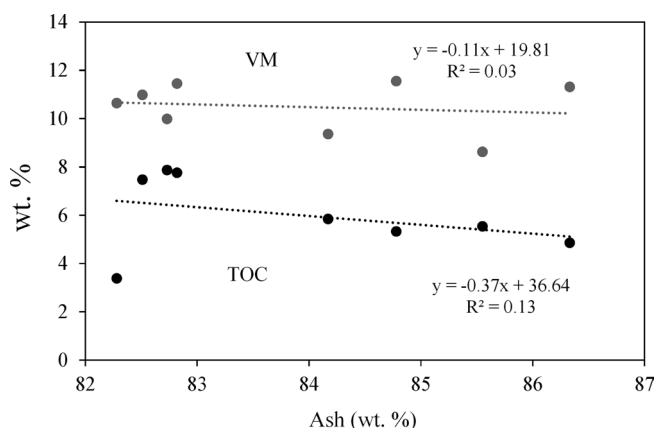


Fig. 4—Relationships between ash vs. volatile matter (VM) and TOC of the shale samples.

Table 2—Proximate analysis results of shale samples.

Sample number	Depth (m)	Formation	IM (wt.%)	Ash (wt.%)	VM (wt.%)	FC (wt.%)	VM <sup>daf</sup> (wt.%)	FC <sup>daf</sup> (wt.%)
1	104.00	Barren Measures	2.60	85.55	8.62	3.23	72.74	27.26
2	149.00	Barren Measures	1.85	84.78	11.55	1.82	86.39	13.61
3	206.00	Barren Measures	1.19	86.33	11.31	1.17	90.63	9.38
4	245.00	Barren Measures	1.94	84.17	9.36	4.53	67.39	32.61
5	227.00	Barakar	1.34	82.82	11.45	4.39	72.29	27.71
6	272.00	Barakar	1.64	82.73	9.99	5.64	63.92	36.08
7	206.00	Barakar	1.52	82.28	10.64	5.56	65.68	34.32
8	241.50	Barakar	1.30	82.51	10.98	5.21	67.82	32.18

IM: In-situ moisture, VM: Volatile matter, FC: Fixed carbon, daf: Dry ash-free basis, wt: Weight.

*al.*, 2015; Mendhe *et al.*, 2015b). The Rock-Eval pyrolysis of the sample gives rise to following important parameters:

- S1 peak denotes any free hydrocarbons that can be volatilized out of the sample without cracking the insoluble organic matter (kerogen). These hydrocarbons are released at isothermal temperature of about 300 °C for 3 minutes, and expressed in milligrams of hydrocarbon per gram of sample (mg HC/g rock).
- S2 signal measures the amount of hydrocarbons (mg HC/g rock) that are expelled from kerogen cracking at temperature programmed pyrolysis. These hydrocarbons are generated by pyrolytic degradation of the organic matter in the samples at temperature of 300 to 550 °C.
- S3 peak determines the released carbon dioxide due to pyrolysis break off between 300 °C and 390 °C expressed in milligrams of CO<sub>2</sub> per gram of rock (mg CO<sub>2</sub>/g rock). CO<sub>2</sub>, as oxygen containing compounds in the samples, are produced from the thermal breakdown of kerogen.
- PI (production index), otherwise known as the transformation ratio [PI = S1/(S1 + S2); mg HC/g rock], denoting ratio of free hydrocarbons to total hydrocarbons. The PI indicates the level of thermal maturation of sample.
- PY (potential yield), also described as 'genetic potential (GP)' of the source rock, of the sample is estimated by summing the quantities of free hydrocarbons and the remaining hydrocarbons (PY = S1 + S2; mg HC/g rock). In other words, it indicates the total amount of oil/gas that might be generated from a sample.
- S2/S3 ratio (described as hydrogen richness) is a measure of amount of hydrocarbons which can be generated from a sample relative to the amount of organic CO<sub>2</sub> released during temperature programming up to 390 °C (Nuñez-betelu & Baceta, 1994).
- TOC (total organic carbon) content is determined by oxidation under air (at temperature of 600 °C) of the residual organic carbon after pyrolysis of the sample. The

- TOC (wt.%) in the sample is then determined by adding residual organic carbon and pyrolyzable organic carbon.
- PC (pyrolyzable carbon) corresponds to the carbon content of hydrocarbons volatilized and pyrolysed during the analysis [PC = 0.083 × (S1 + S2); Claypool & Pimmel, 2001].
- RC (residual carbon) denotes the organic carbon content remaining in the sample after pyrolysis at 600 °C, and is calculated by subtracting PC from TOC.
- HI (hydrogen index) is the normalized S2 value [HI = (S2/TOC) × 100; mg HC/g TOC]; indicating the potential of kerogen in a sample to generate hydrocarbons (oil/gas).
- OI (oxygen index) is related to the amount of oxygen in the kerogen [OI = (S3/TOC) × 100; mg CO<sub>2</sub>/g TOC].
- T<sub>max</sub> (°C) is the temperature (pyrolysis oven temperature) at which the maximum pyrolytic liberation of hydrocarbons (S2) from kerogen is observed, i.e. the temperature at which the maximum amount of hydrocarbons are generated from the sample. T<sub>max</sub> is considered to be a measure of the thermal maturity of organic matter (Hunt, 1996).

Results of Rock-Eval pyrolysis, TOC analysis and various derived parameters of the studied shale samples are presented in Table 3. The free hydrocarbon (S1) values are extremely low in the samples, ranging from 0.25 to 0.88 mg HC/g rock. The remaining hydrocarbon (S2) ranges from 3.10 to 12.54 mg HC/g rock. The S2 value shows the existing potential of a sample to generate hydrocarbons (especially oil) if burial and maturation would continue to completion. While S2 values < 4.0 mg HC/g rock are generally considered to be source rocks with poor generative potential, yields > 4.0 mg HC/g rock are common in known hydrocarbon source rocks. Thus, the obtained S2 values indicate that the studied shales have well to very good source rock potential. The CO<sub>2</sub> generated from organic matter/kerogen of the shales (S3) is found to be in the range of 0.27 to 0.96 mg CO<sub>2</sub>/g rock. The quantity of organic matter in the samples is indicated by the

Table 3—Rock–Eval pyrolysis and TOC results of shale samples.

Sample number	Depth (m)	S1	S2	S3	T <sub>max</sub> (°C)	TOC (wt.%)	S2/S3	HI	OI	PI	PY	PC (wt.%)	RC (wt.%)	Calc. VR <sub>o</sub> %
1	104.00	0.36	7.60	0.27	443	5.54	28.15	137	5	0.05	7.96	0.66	4.88	0.81
2	149.00	0.42	9.63	0.32	442	5.33	30.09	181	6	0.04	10.05	0.83	4.50	0.80
3	206.00	0.37	8.30	0.41	444	4.86	20.24	171	8	0.04	8.67	0.72	4.14	0.83
4	245.00	0.27	4.28	0.58	462	5.84	7.38	73	10	0.06	4.55	0.38	5.46	1.16
5	227.00	0.48	9.47	0.36	441	7.76	26.31	122	5	0.05	9.95	0.83	6.93	0.78
6	272.00	0.88	12.54	0.53	445	7.87	23.66	159	7	0.07	13.42	1.11	6.76	0.85
7	206.00	0.25	3.10	0.61	438	3.38	5.08	92	18	0.07	3.35	0.28	3.10	0.72
8	241.50	0.4	4.20	0.96	459	7.47	4.38	56	13	0.09	4.60	0.38	7.09	1.10

S1: Free hydrocarbons in sample (mg HC/g rock), S2: Remaining hydrocarbons (mg HC/g rock), S3: CO<sub>2</sub> value (mg CO<sub>2</sub>/g rock), T<sub>max</sub>: Maximum temperature of pyrolysis, TOC: Total organic carbon, S2/S3: Hydrocarbon type index, HI: Hydrogen index (mg HC/g TOC), OI: Oxygen index (mg CO<sub>2</sub>/g TOC), PI: Production index (ratio of free hydrocarbons to total hydrocarbons, mg HC/g rock), PY: Potential yield (hydrocarbon generating potential, mg HC/g rock), PC: Pyrolyzable organic carbon, RC: Residual organic carbon, wt: Weight, Calc. VR<sub>o</sub>: Calculated vitrinite reflectance.

TOC content, which varies from 3.38 to 7.87 wt.% (average 6.62 wt.%) and 4.86 to 5.84 wt.% (average 5.39 wt.%) for Barakar and Barren Measures shales, respectively.

The thresholds for the source rock quality are based on hydrogen index values (Peters & Cassa, 1994; Hakimi *et al.*, 2013). All the samples exhibit HI values of < 200 mg HC/g TOC (range: 56–181 mg HC/g TOC, Table 3); signifying that the studied shales are gas-prone. The samples that contain a type III–IV kerogen would be expected to generate gas with HI values < 200, but greater than 50 mg HC/g TOC, whereas samples with HI values > 200 mg HC/g TOC (and < 300 mg HC/g TOC) can generate oil although their main generation products are gas and condensate (Hunt, 1996; Peters & Cassa, 1994; Varma *et al.*, 2015a). The oxygen index (OI) values for the studied samples vary between 5 and 18 mg CO<sub>2</sub>/g TOC. Cross plots of HI and OI values on Van Krevelen diagram demonstrate that the samples are scattered in the kerogen types III and IV mixed area (Fig. 5). Type III kerogen is normally considered to be potential source of wet gas, while type IV kerogen (HI value: < 50 mg HC/g TOC) is generally regarded

as inert, with little (chiefly dry gas) or no hydrocarbon source potential (Tissot & Welte, 1984; Peters, 1986; Ibrahimbas & Riediger, 2004).

The composition of kerogen determines the genetic potential and the amount of hydrocarbons that can be generated during burial of the source deposits. In other words, hydrocarbon generating potential is estimated by measurement of total pyrolytic hydrocarbon yield (PY = S1 + S2). The amount of hydrocarbons released under S2 signals versus TOC contents plot on the model proposed by Langford & Blanc-Valleron (1990) also indicates that the studied shales contain dominantly types III–IV admixed organic materials (kerogens, Fig. 6); suggesting that the shale sequences of both the Barakar and Barren Measures formations have good to excellent potentials of gas source. The obtained potential yield values of hydrocarbons (S1 + S2) varies from 3.35 to 13.42

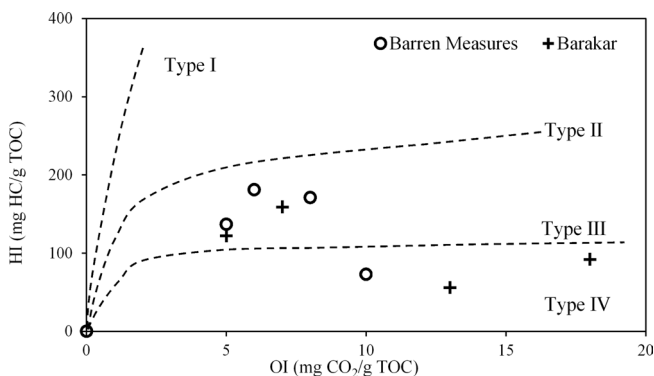


Fig. 5—Van Krevelen (Hydrogen Index vs. Oxygen Index) diagram of the studied shale samples.

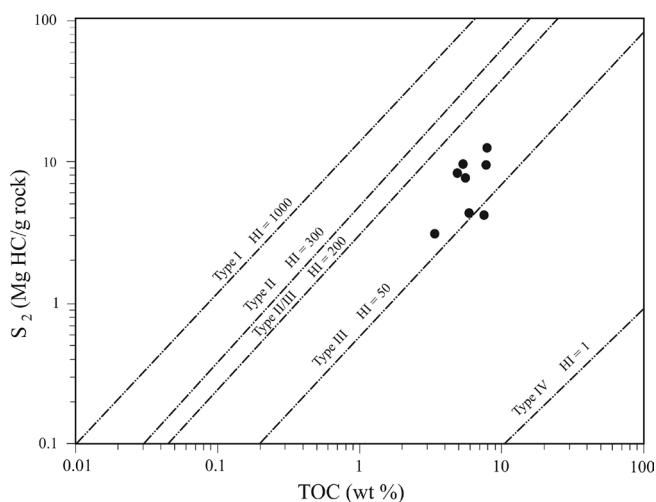


Fig. 6—Relation between TOC and hydrocarbons released under S2 peak of the shale samples.

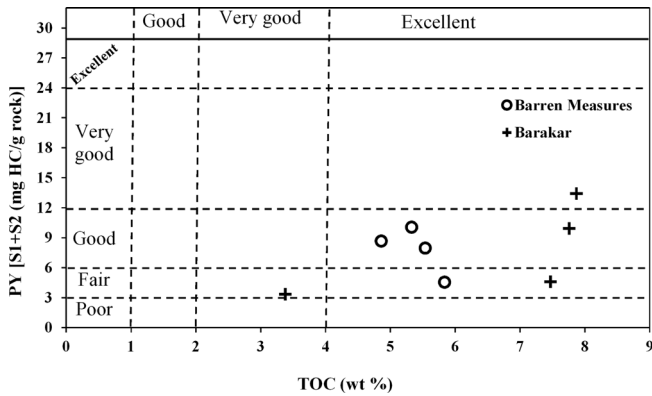


Fig. 7—Relation between hydrocarbon generating potential and TOC content of the shale samples.

mg HC/g rock for the samples; supporting a fair to excellent source for hydrocarbon generation along with a range of TOC contents (Table 3, Fig. 7). S1 + S2 values are generally similar to TOC values. The plot of free hydrocarbons (S1) values vs. TOC contents exhibits of syngenetic hydrocarbons in nature (Fig. 8; Langford & Blanc-Valleron, 1990) for both the Early Permian Barakar and Late Permian Barren Measures shales. The hydrocarbons of both the Lower Gondwana formations under S1 curve appear to be formed during organic maturation stage.

The production index (PI) is significant when it is higher than 0.05–0.1 (Hunt, 1996). The analysed shale samples have an average PI of 0.06, with a maximum value of 0.09 (Table 3). The cross plots of PI value vs. depth of samples indicates that the PI is increased with increasing depth of burial of organic matter (Fig. 9; Barker, 1974). This also entails the increase in PI is mainly due to cracking of the kerogen and to lesser extent, thermal vaporization and cracking as asphaltene, which causes the S2 signals to progressively transform to S1. The ratio of free hydrocarbons to total hydrocarbons (PI values: < 0.1) also indicates that the shale samples are at an immature

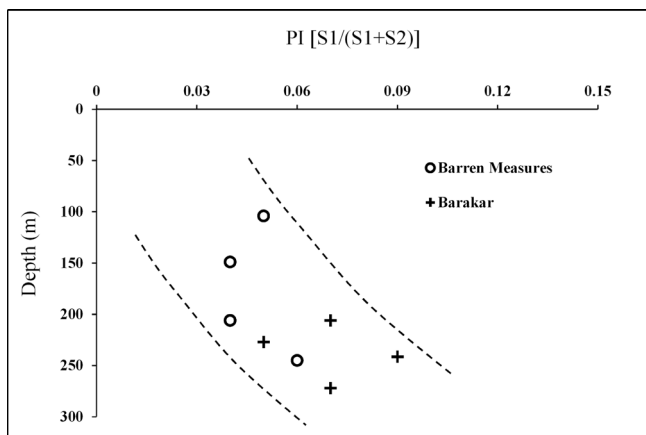


Fig. 9—Relation between production index and depth of the studied shale samples.

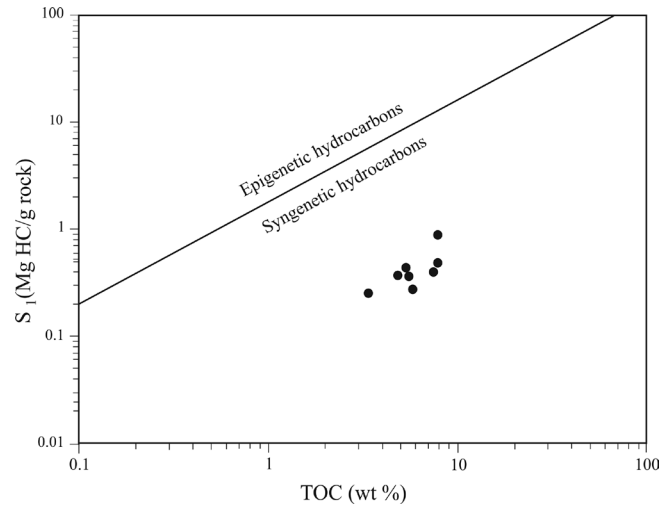


Fig. 8—Relation between TOC and free hydrocarbons (S1) contents of the shale samples.

stage to generate oil, but well-enough to produce gas (Peters & Cassa, 1994; Hunt, 1996; Hazra *et al.*, 2015; Varma *et al.*, 2015b, c). The inter-relationships of some other parameters—residual carbon vs. fixed carbon, pyrolyzed carbon vs. fixed carbon, and S3 vs. ash are seem to be affected by the high ash (mineral matter) yields and narrow range of TOC contents in the studied samples.

The maximum temperature of pyrolysis ( $T_{max}$  value) varies from 438 to 459 °C (av. 446 °C) for the Barakar shales, and from 442 to 462 °C (av. 448 °C) for the Barren Measures shales. This clearly suggests that the studied samples passed the early stage of diagenesis. The  $T_{max}$  value is also used to calculate vitrinite reflectance, to assess rank/maturity level of the sample, as suggested by Jarvie *et al.* (2001; Calc.  $VR_o\% = 0.0180 \times T_{max} - 7.16$ ). The calculated vitrinite reflectance (Calc.

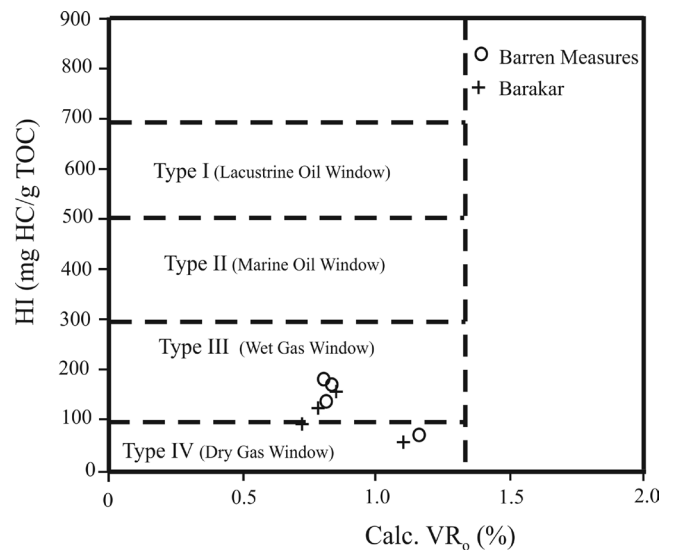


Fig. 10—Hydrogen Index vs. calculated  $VR_o$  plot of the shale samples.

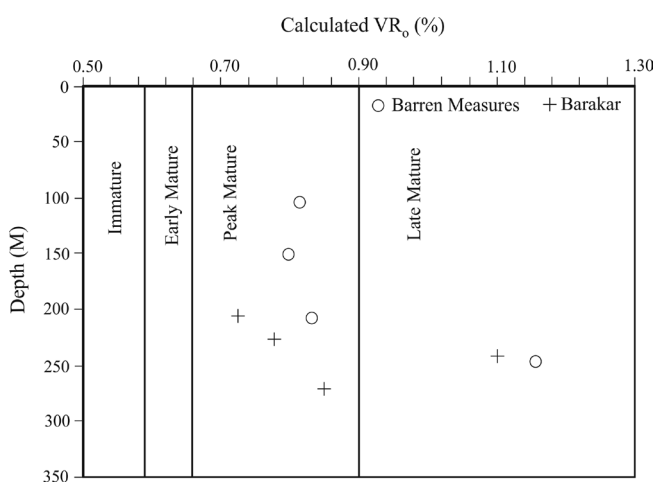


Fig. 11—Relation between depth and calc.  $VR_0$  of the shale samples.

$VR_0$  values of the shales are in the range of 0.72 to 1.16% (Table 3), and are in accordance with the volatile matter yields. The Calc.  $VR_0$  % is plotted against HI (Fig. 10; Ogala, 2011) and this also indicating that all the samples fall in typical gas-prone type III and IV kerogen zones. The correlation between  $T_{max}$  and HI values is also largely pointing towards the input of dominantly types III–IV admixed organic materials.

The cross plots of sample's depth and Calc.  $VR_0$  % suggests that the studied shales are thermally peak to late mature in stage with respect to the gas window (Fig. 11). In this figure, the boundaries of maturity (rank) window in terms of vitrinite reflectance are according to Peters and Cassa (1994). Vitrinite maceral in these samples is too sparse to be of value in determining the thermal maturity, but the  $T_{max}$  values are from 438 to 462 °C; indicating that the samples are thermally immature to over mature with respect to the oil window (Ibrahimbas & Riediger, 2004; Mendhe *et al.*, 2015b). Otherwise, the hydrogen richness (S2/S3) values of the studied shales are higher than 2 and their PI values < 0.1, suggesting that the samples could produce liquid hydrocarbons.

The type and content of minerals present in shale have a significant influence on the behaviour and properties of the shale gas reservoir. Minerals effect may significantly influence the quantity and the composition of pyrolyzates, especially when samples have high clay and carbonate contents (Peters, 1986; Langford & Blanc-Valleron, 1990), such as in the case of the studied shales. Figure 12 shows the Fourier Transform Infrared Spectrometry (FTIR) spectra of shale samples from both the Barren Measures (sample No. 2) and Barakar (sample No. 7) formations of Raniganj Coalfield. The organic and mineralogical (inorganic) compositions of shales are interpreted from diagnostic molecular vibration modes within the spectral region (frequency or wave number: 4000–500  $cm^{-1}$ ). A distinct phase of O–H stretch vibrations between 3750 and 3400  $cm^{-1}$  represents mainly the Phyllo-silicates

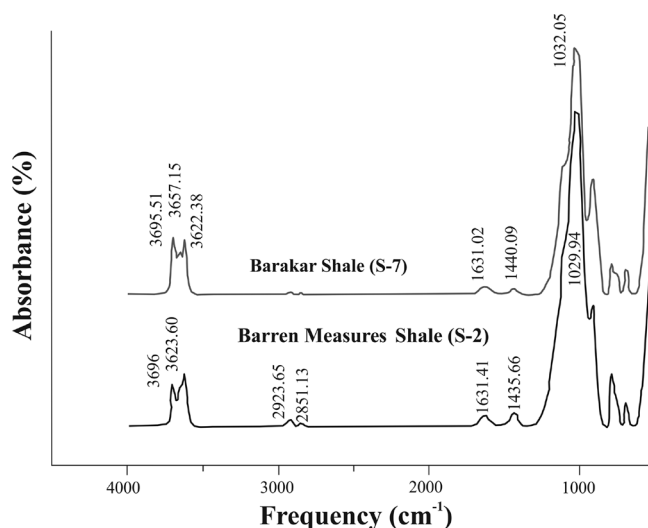


Fig. 12—FTIR spectra of the Barren Measures and Barakar shales.

group (layers of kaolinite, a clay mineral). The absorbance bands within 3000–2800  $cm^{-1}$  display presence of kerogens (organic materials) in shales, which is slightly prominent in the Barren Measures shale than that of the Barakar shale. The absorption band at 1630  $cm^{-1}$  indicates the presence of carbonate/calcite minerals. The peaks 1500–1400  $cm^{-1}$  represents the strong absorption of carbonates due to internal vibration modes of  $CO_3^{2-}$  ions. The absorbance peaks between 1029 and 1032  $cm^{-1}$  shows the abundance of quartz. Spectra of silicates are characterized by Si–O stretching between 1200–800  $cm^{-1}$  (Moenke, 1974; Chen *et al.*, 2014). Abundance of quartz (Si) as compared to clay (Al) points towards the brittle characteristics of shales, which favoured for sufficient micro-facture networks (fracability) in the samples.

Investigation of microstructures along with chemical components of gas is very critical to understand the micro-structural controls on porosity and permeability of a shale deposit. The matrix pore structure of shale gas reservoirs plays an important role in hydrocarbons storage and migration. It is too difficult to characterize accurately because of the predominant portion of nano-pores are associated with clays and organic matters (Bustin *et al.*, 2008). Very few studies have been attempted world over to reconstruct submicro- to micropore structures in shales. Figure 13 illustrates the scanning electron microscopy (SEM) images; showing the variations in submicro- to micropore structures. On the basis of observations under SEM, the pores in the studied shales are classified into four types:

- Inter-granular pores within clastic grains (Fig. 13a)—The clays and minerals forming inter-granular pores are curbed by clastic mineral particles mostly at macro-porous level. They are uneven in pore shape, random in distribution, and are characterized as inter-crystalline pores between quartz and clay minerals. The clastic inter-granular pores are developed in between quartz,

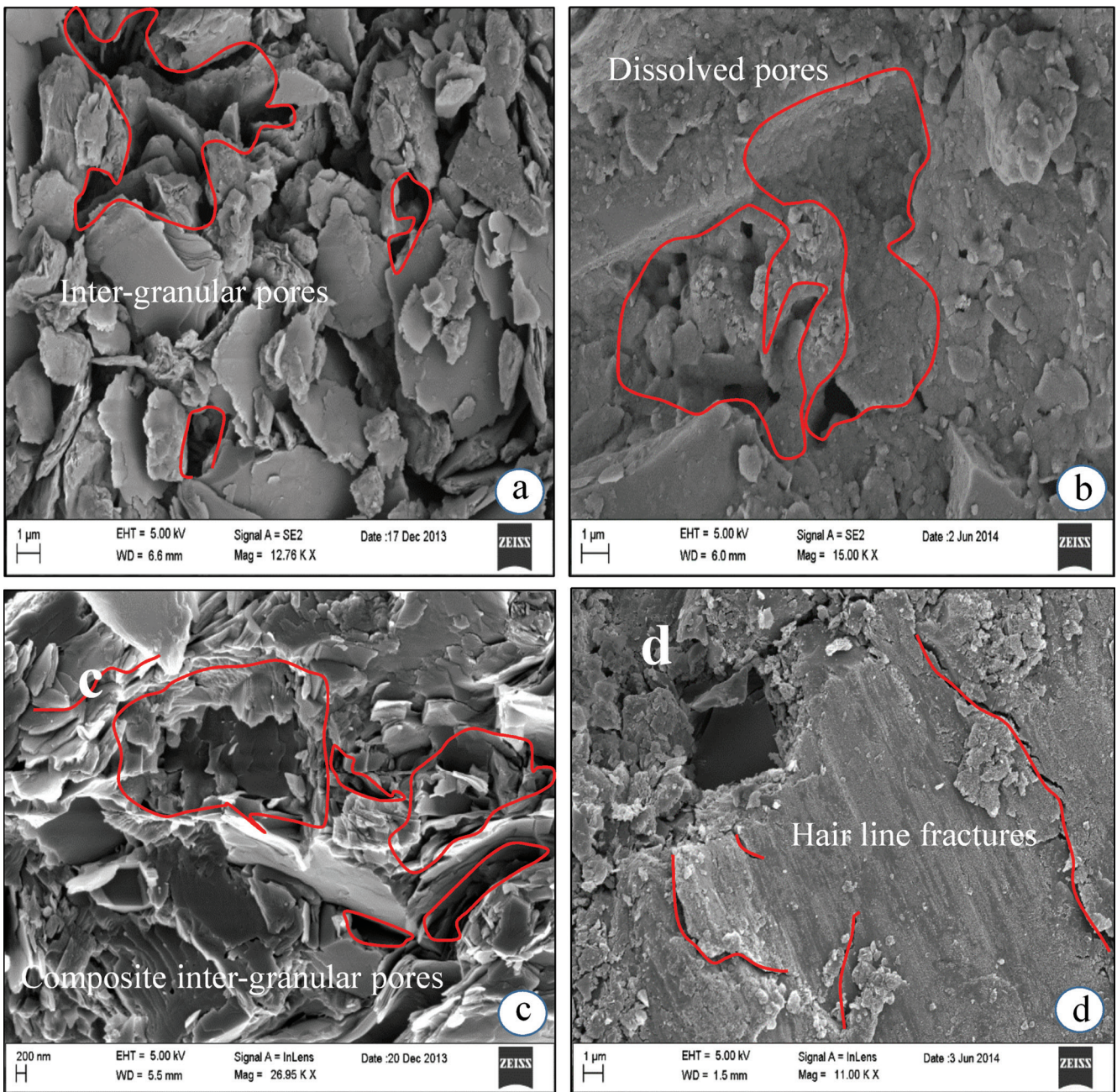


Fig. 13—SEM images of shale samples showing (areas marked in red) inter–granular pores (a), dissolved pores (b), composite inter–granular pores (c), and hair line fractures (d).

feldspar, mica and other rigid particles in sandy/silty laminae. They are irregular to polygonal in shape, and mainly macropores are in micron size (Wang *et al.*, 2014).

- ii) Dissolved pores in feldspar (Fig. 13b)— Dissolved pores or secondary pores are formed by dissolution of clay minerals by interaction with water and solutions present in the horizon. They are very common in calcareous or

sandy shale and feldspar laths. Part of feldspar laths were subjected to strong dissolution, forming dissolved vugs in micron size (Wang *et al.*, 2014).

- iii) Composite inter–granular pores in clay minerals (Fig. 13c)— The weathered muscovite–mica grains formed the thin layered fissile clay minerals which have composite inter–granular pore spaces controlled by irregular structures.

Table 4—Analytical results of surface area, pore size and pore volume for the shale samples.

Sample number	BET multi point Method	BJH Method			DFT Method		
	Surface Area (m <sup>2</sup> /g)	Surface Area (m <sup>2</sup> /g)	Pore Diameter Dv(d) (nm)	Pore Volume (cc/g)	Surface Area (m <sup>2</sup> /g)	Pore width (mode) (nm)	Pore Volume (cm <sup>3</sup> /g)
1	29.381	14.491	3.521	0.029	19.661	3.969	0.033
2	29.675	17.830	2.984	0.040	20.048	3.969	0.041
3	17.376	7.558	2.990	0.012	12.263	1.410	0.016
4	21.632	12.575	3.409	0.028	12.586	3.969	0.029
5	16.973	10.517	3.728	0.022	11.201	3.794	0.022
6	12.897	6.160	2.993	0.010	9.221	1.410	0.013
7	8.104	4.762	3.072	0.014	6.131	3.794	0.013
8	10.243	4.964	3.637	0.014	7.421	3.627	0.016

BET: Brunauer Emmet Teller, BJH: Barret–Joyner–Halenda, DFT: Density Functional Theory.

iv) Hair line micro–fractures (Fig. 13d)— The development of hairline cracks within the shales is caused by stress or pressure exceeding the rock strength.

Characterization of pore structure is of great importance for the percolation mechanism and reservoir evaluation of shale gas (Clarkson *et al.*, 2011). The low–pressure nitrogen (N<sub>2</sub>) adsorption and desorption isotherms and their hysteresis patterns may provide useful evidences regarding the physical sorption mechanism and the pore structures of the shales (Brunauer *et al.*, 1940; Kuila *et al.*, 2012). According to the International Union of Pure and Applied Chemistry (IUPAC) recommendations (Sing *et al.*, 1985), the pores are classified according to their diameter size as– micropores (< 2 nm), mesopores (2–50 nm), and macropores (> 50 nm). The IUPAC has also classified the adsorption isotherms into six types, such as Type I to Type VI, and the desorption isotherms (namely hysteresis patterns) into four types, assigned as H1 to H4.

Figure 14 displays the low–pressure N<sub>2</sub> adsorption and desorption isotherm curves for the studied Barakar and Barren Measures

shales. The obtained shapes of curve suggest Type II and IV isotherms. Type II isotherm indicates macro–porous or non–porous adsorbent, and both monolayer and multilayer adsorptions, whereas Type IV adsorption curve may be characterized to the presence of meso–porous pore structures. The identified H3 hysteresis loop for Barren Measures shale shows the presence of non–rigid aggregates of plate like particles; giving rise to narrow slit–shaped pores, and H2 pattern (for Barakar shale) is attributed to bottle neck pores (de Boer, 1958; Labani *et al.*, 2013; Quantachrome, 2014). It indicates that the pore geometry of the studied shale samples is relatively complex. Further, this essentially implies that mineral matters (as expressed by the ash yields and FTIR spectra) in shales though reduce their sorption capacity, but have some important role in sorption properties (Hazra *et al.*, 2015).

The experimentally measured surface area, following BET (Brunauer Emmet Teller) method, for Barakar and Barren Measures shales varies from 8.104 to 16.973 m<sup>2</sup>/g

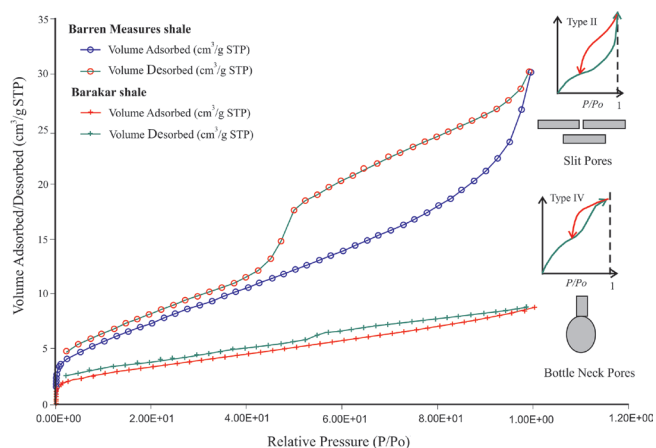


Fig. 14—Low pressure N<sub>2</sub> adsorption–desorption isotherm curves for the shales.

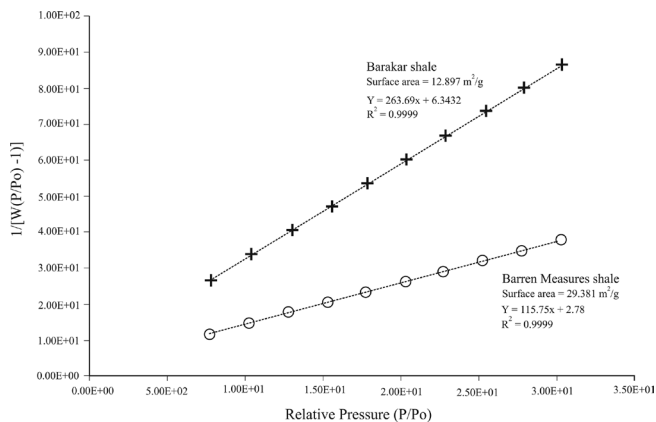


Fig. 15—BET surface plot for the shales of Barakar and Barren Measures formations.

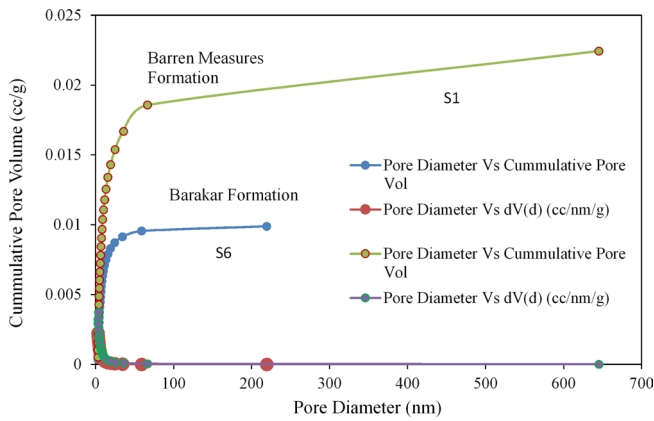


Fig. 16—Pore size distribution by BJH method for the shales of Barakar and Barren Measures formations.

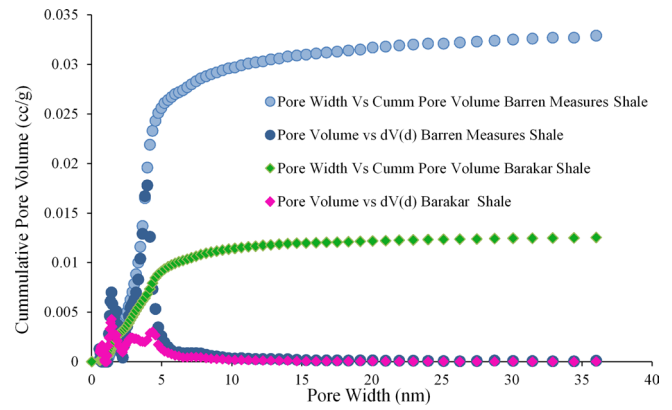


Fig. 17—PSD by DFT method for the shales of Barakar and Barren Measures formations.

and 17.376 to 29.675 m<sup>2</sup>/g, respectively (Table 4). Figure 15 shows a linear trend with a positive intercept over the region of multilayer adsorption, within the approximate P/P<sub>0</sub> (relative pressure) range of 0.05 to 0.30 (Gregg & Sing, 1982; Rouquerol *et al.*, 1999; Kuila *et al.*, 2012; Kuila & Prasad, 2013). The pore size distribution is obtained following the application of BJH (Barrett–Joyner–Halenda) technique; assuming cylindrical pore geometry as shown in the Figure 16. The Barren Measures shale has pore size distribution wide in range from 0 to 700 nm, but majority of the pores are distributed in 0 to 100 nm; indicating abundance of meso– to macropores, which are helpful in more gas sorption capacity. On the contrary, Barakar shale is limited within 0 to 250 nm, and the majority of pores ranges from 0 to 50 nm; signifying dominance of mesopores. Thus, very little numbers of micropores, dominantly lamellar structures, are present in the studied shale organic matter, which is induced by its composition. The lesser amount of micropores measured in the samples is may be due to the non–penetration of N<sub>2</sub> molecules in pores < 2 nm. All these mesopores, macropores, micropores and micro–fractures are connected to natural cracks that form

the network pore system, which may control the storage and flow of gas in the shale reservoir.

Figure 17 presents the cumulative pore volume of the shale samples with respect to pore width using DFT (Density Functional Theory) method. It shows that the shales of Barren Measures have more pore width range and adsorbed cumulative pore volume than those of the Barakar shales. The surface area of shale samples plotted with depth of occurrence scatter graph for depth vs. BET surface area (Fig. 18) shows a negative trend with correlation coefficient R<sup>2</sup> = 0.55; indicating that as depth increases the surface area of the shale decreases. The cross plots of TOC content counter to surface area obtained through BET, BJH and DFT methods demonstrates the negative correlation (Fig. 19); indicating that TOC content do not have major contribution to the amount of surface area in the shales. Whereas, the plot of pore size distribution, obtained by using BJH method, and TOC content exhibits positive correlation (Fig. 20); signifying the role of TOC contents in the development and occurrence of pore distribution in the studied shales.

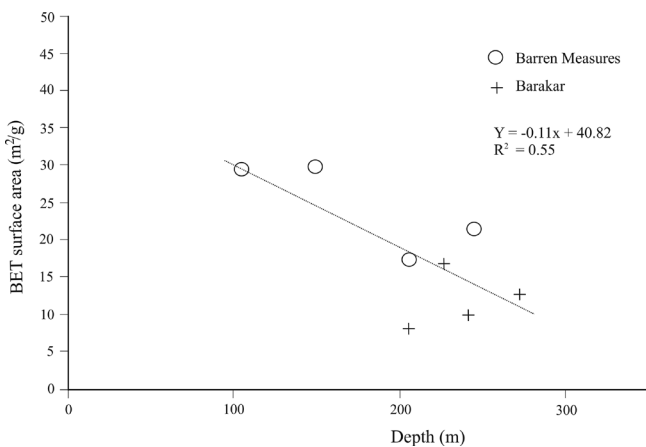


Fig. 18—Relation between depth and BET surface area of the studied shales.

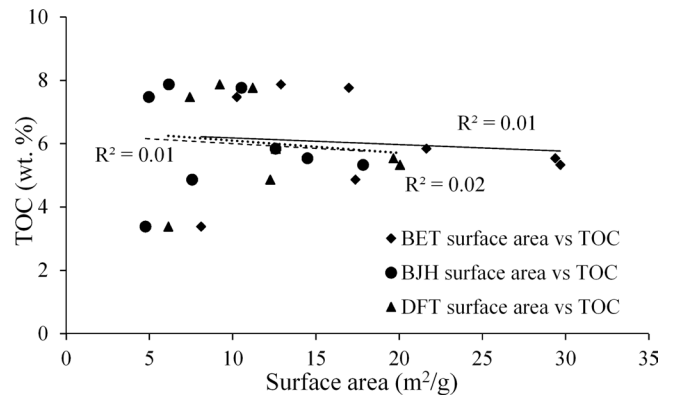


Fig. 19—Relation between TOC and BET, BJH, DFT surface area of the studied shales.

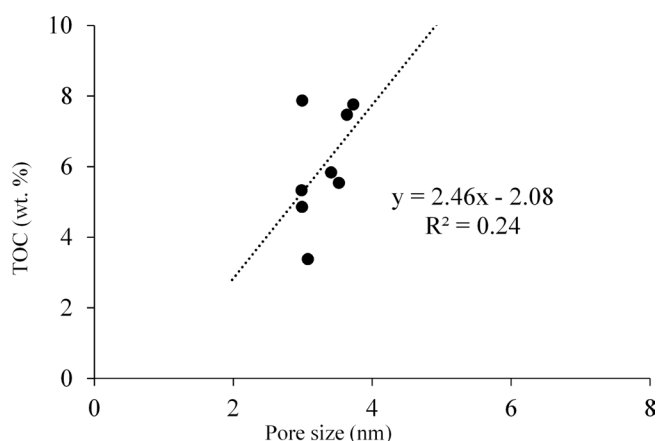


Fig. 20—Relation between BJH pore size distribution and TOC of the studied shales.

Thus, the overall characteristics indicate that the Permian Lower Gondwana shale sequences of Raniganj Coalfield have the potential to generate gaseous hydrocarbon. Rock–Eval pyrolysis, TOC, HI, and adsorption–desorption isotherms data indicated the heterogeneity in Barakar and Barren Measures shales, which is varying laterally. The reason may be attributed to the narrow range of TOC content and sorption capacity for the samples from the Barren Measures Formation as compared to those from the Barakar Formation. However, the sufficient contents of TOC and admixed type III–IV kerogens (organic matters) along with achieved thermal maturity support the occurrence of shale gas accumulations. The findings are in accordance with the earlier observed results of Varma *et al.* (2011; 2014; 2015b, c) and Hazra *et al.* (2015) for the shales from widely apart areas of the Raniganj Basin. Additionally, good fracability (micro–fracture networks), mesopores and macropores are well–developed, thereby the capacity of gas generation and adsorption are significant. The shales of the Barren Measures Formation (Late Permian) have comparatively better characteristics than those of the Barakar Formation (Early Permian), and may be considered as horizon of prospects for shale gas exploitation in the Raniganj Coalfield.

## CONCLUSIONS

An integrated approach of proximate analysis, Rock–Eval pyrolysis, total organic carbon (TOC) contents, and mineral (through FTIR spectroscopy) and pore (under SEM) categorizations along with adsorption–desorption isotherms and surface area evaluation has been applied for the characterization of Permian Lower Gondwana shale deposits from the Raniganj Coalfield (West Bengal, India). The inferences drawn from the data generated on shales of the Early Permian Barakar and the Late Permian Barren Measures formations are complimentary to each other. The following conclusions are drawn with regard to the types of organic

matter, thermal maturity and gas generating potentiality of the studied Lower Gondwana shales:

- The shales are composed predominantly of light and dark grey banded lithotypes; such bands are related to high ash yields. The volatile matter yields are in accordance with the maturity (calculated vitrinite reflectance:  $VR_0$ ) of the shales.
- Significant amount of TOC contents, averaging 6.62 wt.% (in Barakar shale) and 5.59 wt.% (in Barren Measures shale), and pyrolysis data indicate that both the shale sequences are having potentiality of genesis of gas.
- $T_{max}$  and calculated  $VR_0$  values suggest a low degree of organic matter transformation and evolution.
- Inter–relationships between the amount of hydrocarbons (S2) and TOC, the hydrogen index (HI) and oxygen index (OI), the maximum temperature of pyrolysis ( $T_{max}$  value) and HI, and between the calculated  $VR_0$  and HI demonstrate the input of dominantly type III–IV admixed organic materials—a typical gas–prone kerogens.
- FTIR spectra show a distinct phase of O–H stretch vibrations; representing mainly the Phyllo–silicates group (layers of kaolinite). In addition, a greater content of clay is also indicated.
- The absorbance bands within the frequencies 3000–2800  $cm^{-1}$  display presence of organic matter (kerogen) in shales, which is slightly prominent in Barren Measures shale than that of the Barakar shale.
- The shales contain mostly mesopores, macropores, slit–pores and very little micropores. Further, the pores are classified into four types– (i) inter–granular pores, (ii) dissolve pores, (iii) composite inter–granular pores, and (iv) hair line micro–fractures, which are helpful in storage and migration of shale gas.
- Adsorption–desorption isotherms provided the more comprehensive pore size distribution in shales with relatively complex pore geometry; mainly slit–shaped pores in the Barren Measures shales and bottle neck pores in the Barakar shales.
- The pore size distribution suggested multi–modal with a broad peak ranges in the studied shales. The pore volume is predominantly occupied by mesopores, and the main specific surface area is dominated by the macro– and mesopores.
- The measured BET multipoint surface areas signified that the Barren Measures shales have relatively more gas (methane) sorption capacity than that of the Barakar shales.

**Acknowledgements**—We are thankful to the Director, CSIR–CIMFR Dhanbad for granting permission to publish this paper. We are also grateful to Ministry of Coal, Govt. of India for funding Grant–in–Aid S & T Project of shale gas potentiality evaluation of Damodar Basin of India.

## REFERENCES

- Barker C 1974. Pyrolysis techniques for source rock evaluation. *American Association Petroleum Geologists Bulletin* 58: 2349–2361.
- BIS 1995. Methods of Test for Coal and Coke (second revision of IS: 1350). Part I, Proximate analysis. Bureau of Indian Standard, pp. 1–29.
- Blanford WT 1861. On the geological structure and relations of the Raniganj Coalfield, Bengal. *Memoir Geological Survey of India* 3 (Part I), 118p.
- Brunauer S, Deming LS, Deming WS & Teller E 1940. On a theory of the Vanderwaals adsorption of gases. *Journal of American Chemical Society* 62: 1723–1732.
- Bustin RM, Bustin AMM, Cui A, Ross D & Pathi VM 2008. Impact of shale properties on pore structure and storage characteristics. SPE Shale Gas Production Conference (November 16–18), Fort Worth, Texas, USA, <http://dx.doi.org/10.2118/119892-MS>.
- Chen Y, Furmann A, Mastalerz M & Schimmelmann A 2014. Quantitative analysis of shales by KBr-FTIR and micro-FTIR. *Fuel* 116: 538–549.
- Clarkson CR, Jensen JL & Blasingame TA 2011. Reservoir engineering for unconventional gas reservoirs: What do we have to consider. SPE North American Unconventional Gas Conference and Exhibition (June 14–16), The Woodlands, Texas, USA, [http://www.pe.tamu.edu/blasingame/data/0\\_TAB\\_Public/TAB\\_Publications/SPE\\_145080\\_\(Clarkson\)\\_Res\\_Eng\\_Uncon\\_Reservoirs.pdf](http://www.pe.tamu.edu/blasingame/data/0_TAB_Public/TAB_Publications/SPE_145080_(Clarkson)_Res_Eng_Uncon_Reservoirs.pdf).
- Claypool G & Pimmel A 2001. Introduction to shipboard organic geochemistry on the JOIDES Resolution. ODP Technical Note 30. Web: <<http://www-odp.tamu.edu/publications/notes/tn30/INDEX.HTM>>
- Claypool GE & Reed PR 1976. Thermal analysis technique for source rock evaluation: Quantitative estimate of organic richness and effects of lithologic variation. *American Association of Petroleum Geologists Bulletin* 60: 608–626.
- Clementz DM, Demaison GJ & Daly AR 1979. Well site geochemistry by programmed pyrolysis. *Proceedings of 11<sup>th</sup> Annual Offshore Technology Conference, Houston (OTC 3410)* 1: 465–470.
- de Boer JH 1958. The structure and properties of porous materials. Butterworths, London, 68p.
- Dutt AB (Ed.) 2003. Coalfields of India—Coal resources of West Bengal. *Bulletin of Geological Survey of India, Series A (No. 45)* 5: 23–96.
- Ekweozor CM & Gormly JR 1983. Petroleum geochemistry of Late Cretaceous and Early Tertiary shales penetrated by Akukwa-2 well in the Anambra Basin, Southern Nigeria. *Journal of Petroleum Geology* 6: 207–216.
- Espitalié J, Laporte JL, Madec M, Marquis F, Leplat P & Paulet J 1977. Methode rapide de caracterisation des roches meres, de leur potentiel petrolier et de leur degre d'evolution. *Review of Institute Petroleum* 32: 23–45.
- Espitalié J, Marquis F & Barsony I 1984. Geochemical logging. *In: Voorhees KJ (Editor)—Analytical pyrolysis—Techniques and applications*, Boston, Butterworth, pp. 276–304.
- Fox CS 1928. Barakar—Ironstone shale boundary near Begunia and Raniganj—Panchet boundary near Asansol, Raniganj Coalfield. *Record Geological Survey of India, Part 4*, 60: 363–366.
- Gee ER 1932. The geology and coal resources of Raniganj Coalfield. *Memoir Geological Survey of India* 61: 1–187.
- Ghosh SC 2002. The Raniganj Coal Basin: An example of an Indian Gondwana rift. *Sedimentary Geology* 147: 155–176.
- Gregg SJ & Sing KSW 1982. Adsorption, surface area and porosity. 2<sup>nd</sup> Edition, Academic Press, New York, 303p.
- Guarone M, Rossi F, Negri E, Grassi C, Genazzi D & Zennaro R 2012. An unconventional mindset for shale gas surface facilities. *Journal of Natural Gas Science and Engineering* 6: 14–23.
- Guo Y & Bustin RM 1998. Micro-FTIR spectroscopy of liptinite macerals in coal. *International Journal of Coal Geology* 36: 259–275.
- Gupta S, Mondal D & Bardhan A 2012. Geochemical provenance and spatial distribution of fluoride in groundwater in parts of Raniganj Coalfield, West Bengal, India. *Archives Applied Science Research* 4(1): 292–306.
- Hakimi MH, Abdullah WH, Sia SG & Makeen YM 2013. Organic geochemical and petrographic characteristics of Tertiary coals in the northwest Sarawak, Malaysia: implications for palaeoenvironmental conditions and hydrocarbon generation potential. *Marine Petroleum Geology* 48: 31–46.
- Hazra B, Varma AK, Bandopadhyay AK, Mendhe VA, Singh BD, Saxena VK, Samad SK & Mishra DK 2015. Petrographic insights of organic matter conversion of Raniganj Basin shales, India. *International Journal of Coal Geology* 150–151: 193–209.
- Hill RJ, Jarvie DM, Zumberge J, Henry M & Pollastro RM 2007. Oil and gas geochemistry and petroleum systems of the Fort Worth Basin. *American Association Petroleum Geologists Bulletin* 91: 445–473.
- Horsfield B 1985. Pyrolysis studies in petroleum exploration. *In: Brooks J & Welte D (Editors)—Advances in Petroleum Geochemistry* 1: 247–298.
- Hunt JM 1996. *Petroleum Geochemistry and Geology*. 2<sup>nd</sup> Edition, W.H. Freeman and Company, New York, 743p.
- Ibrahimbas A & Riediger C 2004. Hydrocarbon source rock potential as determined by Rock-Eval 6/TOC pyrolysis, Northeast British Columbia and Northwest Alberta. *Resource Development and Geoscience Branch Summary of Activities, British Columbia Ministry of Energy and Mines*, pp. 7–18.
- Jarvie DM, Claxton BL, Henk F & Breyer JT 2001. Oil and shale gas from the Barnett Shale, Ft. Worth Basin, Texas. *American Association of Petroleum Geologists Bulletin* 85: A100 (No. 13 supplement)
- Jarvie DM, Hill RJ & Pollastro RM 2005. Assessment of the gas potential and yields from shales: The Barnett Shale Model. *Oklahoma Geological Survey Circular* 110: 37–50.
- Jarvie DM, Hill RJ, Ruble TE & Pollastro RM 2007. Unconventional shale-gas systems: The Mississippian Barnett Shale of north central Texas as one model for thermogenic shale-gas assessment. *American Association of Petroleum Geologists Bulletin* 91: 475–499.
- Kuila U & Prasad M 2013. Specific surface area and pore-size distribution in clays and shales. *Geophysical Prospecting* EAGE 61: 341–362.
- Kuila U, Prasad M, Derkowski A & McCarty DK 2012. Compositional controls on mudrock pore-size distribution: An example from Nibrara Formation. SPE Annual Technical and Exhibition (October 8–10), San Antonio, USA, <http://dx.doi.org/10.2118/160141-MS>.
- Labani MM, Rezaee R, Saeedi A & Hinai AA 2013. Evaluation of pore size spectrum of gas shale reservoirs using low pressure nitrogen adsorption, gas expansion and mercury porosimetry: A case study from the Perth and Canning Basins, western Australia. *Journal of Petroleum Science and Engineering* 112: 7–16.
- Lafargue E, Marquis F & Pillot D 1998. Rock-Eval-6 applications in hydrocarbon exploration, production and soil contamination studies. *Oil Gas Science Technology* 53: 421–437.
- Langford FF & Blanc-Valleron MM 1990. Interpreting Rock-Eval pyrolysis data using graphs of pyrolyzable hydrocarbons vs. total organic carbon. *American Association of Petroleum Geologists Bulletin* 74: 799–804.
- Larter SR & Douglas AG 1982. Pyrolysis methods in organic geochemistry: An overview. *Journal of Applied Pyrolysis* 4: 1–19.
- Li S, Dong M, Li Z, Huang S, Qing H & Nickel E 2005. Gas breakthrough pressure for hydrocarbon reservoir seal rocks: Implications for the security of long-term CO<sub>2</sub> storage in the Weyburn field. *Geofluids* 5: 326–334.
- Loucks RG, Reed RM, Ruppel SC & Jarvie DM 2009. Morphology, genesis and distribution of nanometer-scale pores in siliceous mudstones of the Mississippian Barnett Shale. *Journal of Sedimentary Research* 79: 848–861.
- Majumdar AK, Banerjee SP & Das AK 1977. Report on the exploratory drilling in Poradiha area, Raniganj Coalfield, Bankura and Purulia districts, West Bengal. Progress Report, Geological Survey of India (unpublished).
- Mendhe VA, Mishra S, Kamble AD, Bannerjee M, Mukherjee S, Kumar V & Sinha A 2015a. Shale gas and emerging energy resource: Prospects in India. *Indian Mining and Engineering Journal* 54: 21–31.
- Mendhe VA, Kamble AD, Bannerjee M, Mishra S, Mukherjee S & Mishra P 2015b. Evaluation of shale gas reservoir in Barakar and Barren Measures formations of North and South Karanpura coalfields, Jharkhand. *Journal Geological Society of India* (in press).
- Moenke HHW 1974. Silica, the three-dimensional silicates, borosilicates and

- beryllium silicates. *In*: Farmer VC (Editor)—Infrared spectra of minerals, Mineralogical Society, London, pp. 365–382.
- Mukhopadhyay G, Mukhopadhyay SK, Roychowdhury M & Parui PK 2010. Stratigraphic correlation between different Gondwana basins of India. *Journal of Geological Society of India* 76: 251–266.
- Nicholas BH, Katherine HF, Richard DP, Timothy SW & Gareth DM 2004. The character and origin of lacustrine source rocks in the Lower Cretaceous synrift section, Congo Basin, West Africa. *American Association of Petroleum Geologists Bulletin* 88: 1163–1184.
- Núñez-betelu L & Baceta JI 1994. Basics and application of Rock–Eval/TOC Pyrolysis: An example from the uppermost Paleocene/lowermost Eocene in the Basque Basin, Western Pyrenees. *San Sebastian* 46: 43–62.
- Ogala JE 2011. Hydrocarbon potential of the Upper Cretaceous coal and shale units in the Anambra Basin, Southeastern Nigeria. *Petroleum and Coal* 53: 35–44.
- Painter PC, Snyder RW, Starsinic M, Coleman MM, Kuehn DW & Davis A 1981. Concerning the applications of FTIR to the study of coal: A critical assessment of band assignments and the application of spectral analysis programs. *Applied Spectroscopy* 35: 475–485.
- Painter PC, Starsinic M & Coleman MM 1985. Determination of functional groups in coal by Fourier transform interferometry. *In*: Ferraro JR & Basile LJ (Editors)—Fourier Transform Infrared Spectroscopy, vol. 4, Academic Press, New York, pp. 169–241.
- Peters KE 1986. Guidelines for evaluating petroleum source rock using programmed pyrolysis. *American Association of Petroleum Geologists Bulletin* 70: 318–329.
- Peters KE & Cassa MR 1994. Applied source rock geochemistry. *In*: Magoon LB & Dow WG (Editors)—The petroleum system from source to trap, American Association of Petroleum Geologists Memoir 60: 93–120.
- Quantachrome 2014. Characterizing porous materials and powders—AutosorbIQ and ASiQwin Gas Sorption System operating manual. volume II: 199–426.
- Rouquerol F, Rouquerol J & Sing K 1999. Adsorption by powders and porous solids: Principles, methodology and application. ISBN 0–12–598920–2, Academic Press, London, 465p.
- Rowe HD, Loucks RG, Ruppel SC & Rimmer SM 2008. Mississippian Barnett Formation, Fort Worth Basin, Texas: Bulk geochemical inferences and Mo–TOC on the severity of hydrographic restriction. *Chemical Geology* 257: 16–25.
- Schlömer S & Krooss BM 1997. Experimental characterization of the hydrocarbon sealing efficiency of cap rocks. *Marine and Petroleum Geology* 14: 565–580.
- Sing KS, Everett DH, Haul RAW, Moscou L, Pierotti RA, Roquerol J & Siemieniowska T 1985. Reporting physisorption data for gas/solid systems with special reference to the determination of surface area and porosity. *Pure Applied Chemistry* 57: 603–619.
- Strapoc D, Mastalerz M, Schimmelmann A, Drobnik A & Hasenmueller NR 2010. Geochemical constraints on the origin and volume of gas in the New Albany Shale (Devonian–Mississippian), eastern Illinois Basin. *American Association of Petroleum Geologists Bulletin* 94: 1713–1740.
- Sykes R & Snowdon LR 2002. Guidelines for assessing petroleum potential of coaly source rocks using Rock–Eval pyrolysis. *Organic Geochemistry* 33: 1441–1455.
- Tissot BP & Welte DH 1984. *Petroleum Formation and Occurrence*. 2<sup>nd</sup> Edition, Springer–Verlag, Berlin, Heidelberg, New York, Tokyo, 669p.
- Varma AK, Biswal S, Hazra B, Mendhe VA, Misra S, Samad SK, Singh BD, Dayal AM & Mani D 2015a. Petrographic characteristics and methane sorption dynamics of coal and shaly–coal samples from Ib Valley Basin, Odisha, India. *International Journal of Coal Geology* 141–142: 51–62.
- Varma AK, Chinara I, Mendhe VA & Singh BD 2011. Hydrocarbon generation evaluation through Rock–Eval pyrolysis—A case study of Raniganj coal basin, West Bengal, India. *In*: Varma OP *et al.* (Editors)—Proceedings of 17<sup>th</sup> Convention Indian Geological Congress & International Conference New Paradigms of Exploration Sustainable Mineral Development, Dhanbad, pp. 475–483.
- Varma AK, Hazra B, Mendhe VA, Chinara I & Dayal AM 2015b. Assessment of organic richness and hydrocarbon generation potential of Raniganj Basin shales, West Bengal, India. *Marine and Petroleum Geology* 59: 480–490.
- Varma AK, Hazra B, Samad SK, Panda S & Mendhe VA 2014. Methane sorption dynamics and hydrocarbon generation of shale samples from West Bokaro and Raniganj basins, India. *Journal of Natural Gas Science Engineering* 21: 1138–1147.
- Varma AK, Khatun M, Mendhe VA, Hazra B, Singh BD & Dayal AM 2015c. Petrographic characterization and Langmuir volume of shales from Raniganj coal basin, India. *Journal of Geological Society of India* 86: 283–294.
- Wang X, Gao S & Gao C 2014. Geological features of Mesozoic lacustrine shale gas in south of Ordos Basin, NW China. *Petroleum Exploration and Development* 41: 326–337.
- Ward CR 2002. Analysis and significance of mineral matter in coal seams. *International Journal of Coal Geology* 50: 135–168.
- Yang F, Ning Z & Liu H 2014. Fractal characteristics of shales from a shale gas reservoir in the Sichuan Basin, China. *Fuel* 115: 378–384.
- Yuguang H, Sheng HE, Jizheng YI, Baiqiao Z, Xuehui C, Yi W, Jiankun Z & Chunyang C 2014. Effect of pore structure on methane sorption potential of shales. *Petroleum Exploration and Development* 41: 272–281.
- Zhang T, Ellis GS, Ruppel SC, Milliken K & Yang R 2012. Effect of organic matter type and thermal maturity on methane adsorption in shale–gas system. *Organic Geochemistry* 47: 120–131.